PHYSICAL REVIEW B VOLUME 27, NUMBER 9 1 MAY 1983

# Thermal-relaxation studies of the stability of amorphous structures in zirconium-based superconducting alloys

S. J. Poon
*Department of Physics, University of Virginia, Charlottesville, Virginia 22901*
(Received 20 December 1982)

The superconducting transition temperature $T_c$ of amorphous $Zr_2X$ ($X$=Co, Ni, Pd) and $Zr_3X$ ($X$=Ni, Pd, Rh) alloys annealed isothermally below their crystallization temperatures is studied as a function of annealing time (up to ~20—100 h). Upon annealing, $T_c$ is always found to decrease below its value in the as-quenched state. The major portion of $T_c$ depression is attributed to the relaxation of "quenched-in" strains. Alloys of $Zr_2Co$, $Zr_2Ni$, $Zr_2Pd$, and $Zr_3Rh$ which undergo polymorphous crystallization ($P$ alloys) show trends of saturation in $T_c$. On the other hand, for $Zr_3Ni$ and $Zr_3Pd$ alloys which crystallize eutectically ($E$ alloys), saturation in $T_c$ is only observed at relatively low annealing temperatures over rather short intervals of annealing time. The results are attributed to the stability and instability of the "equilibrium" amorphous structures in the $P$ and $E$ alloys, respectively. It is conjectured that instability in the $E$ alloys leads to initial microscopic phase separation, the homogeneity of which is evidenced by results on transition width and flux pinning measurements. All homogeneous samples exhibit very weak flux-pinning force of about $10^4$ N/m$^3$ at 1.5 K. Prolonged annealing of $E$ alloys leads to eutectic decomposition. Predictions derived from a simple "proximity-effect" model are consistent with the present findings.

## I. INTRODUCTION

The variability in many of the properties of metallic glasses subject to post-quench annealing is largely due to the subtle structural variations in these highly degenerate systems. Associated with these systems are the multiple local free-energy minima, the existence of which is commonly demonstrated by the reversibility in the many physical properties upon thermal relaxation. Experiments performed on reversible relaxation in glassy alloys include magnetic,[1,2] structural,[3,4] transport,[5] calorimetric,[6,7] acoustic,[8] and superconductive[9,10] measurements. In addition to the reversible transition between "metastable" amorphous states created at different annealing temperatures,[9] reversibility among "equilibrium" amorphous states characterized by "saturation" in some of the physical properties have also been observed in some amorphous magnetic and superconductive alloys.[3,10,11] On the other hand, it was noted that in superconductive $Zr_3Pd$ alloys, saturation in $T_c$ was never achieved in the temperature range of 180—280 °C.[10] Prolonged annealing ultimately led to eutectic decomposition into $\alpha$-Zr and $Zr_2Pd$. One would naturally wonder about the nature of the intermediate states prior to macroscopic phase separation and the stability of the equilibrium amorphous structures with respect to the other competing phases. To ensure that the existence of intermediate phases is not due to the presence of "quenched-in" crystallites, appropriate tests must be made to study the degree of homogeneity of the samples. The growth of quenched-in crystallites in samples annealed below their glass temperatures can sometimes alter their physical properties in a rather significant way. It was found that the presence of crystallites in amorphous superconductors could indeed enhance the transition width, upper and lower critical fields, and critical current above those obtained in homogeneous samples.[12,13] As a result, superconductivity provides a rather sensitive tool for probing the microscopic states of amorphous alloys.

It is the purpose of this paper to study the stability of equilibrium amorphous states in binary alloys, using superconducting transition temperature $T_c$ to characterize the amorphous states. The occurrence of saturation in $T_c$ upon isothermal annealing will be used as sufficient evidence for the existence of equilibrium states, according to the discussion presented above. The homogeneity of the samples will be discussed in the light of transition width and flux pinning force. Alloy systems with different superconducting properties in their corresponding crystalline counterparts are being used to provide a variety of atomic short-range orders and electronic

 

structures in the amorphous phase. This systematic study might lead to a better understanding of the effect of annealing on $T_c$. Finally, a simple model based on the proximity effect is employed to treat phase separation in amorphous systems. The format of this paper is as follows. In Sec. II, experimental procedures are given. Section III presents experimental results and discussion. Section IV is the summary and conclusion.

## II. EXPERIMENTAL PROCEDURES

Alloys of composition $Zr_2Co$, $Zr_2Ni$, $Zr_3Ni$, $Zr_2Pd$, $Zr_3Pd$, and $Zr_3Rh$ were used in this study. Amorphous ribbons were prepared and analyzed according to the methods outlined in Ref. 12. Sections of ribbons of size $\sim 25\ \mu m \times 1$ mm $\times 15$ mm were used as samples in the superconducting measurements. Critical temperature was measured resistively in a four-point probe. The current density was $\sim 10^5$ A/m$^2$. Temperature was monitored using both a carbon resistor and a Hg manometer with resolution of $\sim 2$ mK. The variation of $T_c$ along a given ribbon was found to be less than 5 mK. Both as-quenched and annealed samples were electropolished prior to critical current measurement. The electrolyte was made from a solution of 1 part perchloric acid and 4 parts ethyl alcohol. The electropolishing was carried out at temperatures of $-20\,^{\circ}$C. Critical current measurement was performed in a magnetic field up to $\sim 40$ kOe. A voltage signal of $\sim 1-2\ \mu$V across the voltage leads was used as a criterion for the determination of critical current.

Sample strips were annealed in thin-wall Pyrex tubes repeatedly evacuated and flushed with argon gas. Excess ribbons about 20 times the size of a sample strip and strips of titanium were placed within the capsule to getter oxygen. The furnace temperature was controlled to within 2 K. After heat treatment the samples were cooled rapidly by moving the capsule from the furnace to water. The annealed samples were routinely scanned by a standard x-ray diffractometer. For isothermal annealing, the same sample strips were used to study its $T_c$ dependence on annealing time. The "additive" annealing effect was checked by measuring several strips of the same ribbons annealed at various lengths of time. The results were almost identical. At least two strips were used for each isothermal annealing.

## III. RESULTS AND DISCUSSION

### A. Homogeneity of samples and transition width

It usually takes about 10—100 h of annealing to establish a definite trend in the $T_c$ behavior. Therefore, caution must be taken to avoid crystallization, phase separation, and possible gaseous contamination in the samples. The effect of phase separation and crystallization on the transition width $\Delta T_c$ and flux pinning force will be discussed in the following sections. To minimize the possible influence on the results due to gaseous contamination and quenched-in surface layers of oxides and crystallites the thickness of which is typically about 10 nm or less,[14] maximum annealing time on all samples was limited to about 200 h. Under these conditions, a criterion based on the transition width $\Delta T_c$ defined by the 0% (i.e., zero resistance) and 90% points on the resistivity curve is used to describe the homogeneity of the samples. In the absence of inhomogeneities, the paraconductivity discussed by Aslamazov and Larkin[15] yields a transition width $\Delta T_c$ given by

$$\Delta T_c = 0.1811 \rho_0^2 T_c^2 H'_{c2}(T_c)\,, \tag{1}$$

where $\rho_0(\Omega\,\text{cm})$ is the normal-state resistivity and $H'_{c2}(\text{Oe/K}) = [dH_{c2}(T)/dT]_{T=T_c}$ is the upper critical field slope at $T_c$. The predicted and measured values of $\Delta T_c$ are tabulated in Table I. In view of the limitations on the accuracy and resolution ($\sim 2$ mK) of the temperature sensors, the agreement is quite good. On the other hand, in inhomogeneous

TABLE I. Comparison between theoretically predicted transition widths and experimental values.

| Alloys | As quenched $T_c$ (K) | $\rho_0$ ($10^{-6}$ Ω cm) | $[dH_{c2}(T)/dT]_{T=T_c}$ (kOe/K) | Predicted $\Delta T_c$ ($10^{-3}$ K) | Data $\Delta T_c$ ($10^{-3}$ K) |
|---|---|---|---|---|---|
| $Zr_2Co$ | 3.00 | 180 | 32.7[a] | 1.73 | ~5 |
| $Zr_2Ni$ | 2.77 | 170 | 28.6[a] | 1.15 | ~4 |
| $Zr_3Ni$ | 3.35 | 170 | 33.4[b] | 1.96 | ~5 |
| $Zr_2Pd$ | 2.36 | 175 | 28.5[b] | 0.89 | ~4 |
| $Zr_3Pd$ | 2.96 | 180 | 30.2[b] | 1.55 | ~4 |
| $Zr_3Rh$ | 4.30 | 230 | 31.8[b] | 5.63 | ~5 |

[a]Z. Altounian and J. O. Strom-Olsen (unpublished).
[b]Reference 13 and present data.

samples $\Delta T_c$ can be an order of magnitude higher than the predicted values.[12] In what follows, a transition width of ~4–7 mK for the present alloys will be taken as characteristic of samples which are homogeneous on a spatial scale of less than the zero temperature coherence length $\xi(0)$.

### B. Effect of isothermal annealing on $T_c$

Figures 1 and 2 show the dependence of $T_c$ as a function of annealing time $t_a$ at various annealing temperatures $T_a$ for amorphous $Zr_3Pd$ and $Zr_3Rh$ samples, respectively. The crystallization temperatures were found to be ~673 K for $Zr_3Pd$ (Ref. 16) and ~730 K for $Zr_3Rh$.[17] Thus the maximum annealing temperatures are ~150 and ~ 90 K below the crystallization temperatures for $Zr_3Pd$ and $Zr_3Rh$, respectively. There is a tendency, however, for the amorphous phase in $Zr_3Pd$ to phase separate (or crystallize) when the samples are being annealed at 523 K for only more than ~5 h or at 488 K for more than ~ 12 h. This is characterized by significant degradation in $T_c$ ($<2.3$ K) and drastic increase in $\Delta T_c$ ($>100$ mK). Prolonged annealing leads to crystallization into $\alpha$-Zr and $Zr_2Pd$. No tendency towards saturation in $T_c$ is observed for $T_a \geq 453$ K. On the other hand, definite trends of saturation in $T_c$ can be seen in the $Zr_3Rh$ samples. This is notedly marked by the "convergence" in the family of $T_c(t_a)$ curves. To perform a routine test for the existence of equilibrium amorphous phase, cyclic annealing is carried out between 553 K for 40 h and 643 K for 30 min (Fig. 2). At the end of each annealing at 553 K, the equilibrium $T_c$ value is reproduced. The result is typical of the reversibility of transitions between equilibrium amorphous structures.[3,11] In view of the instability of the amorphous structures in $Zr_3Pd$, annealing is also being carried out at lower temperatures of 413 and 433 K.

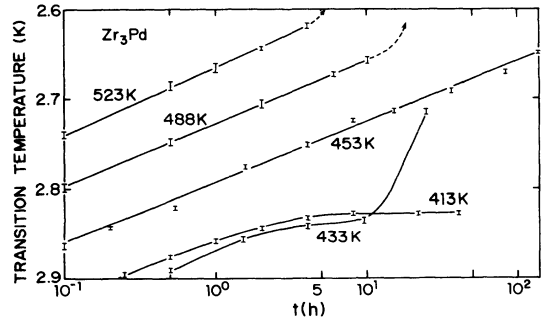


FIG. 1. Superconducting transition temperature as a function of annealing time at different annealing temperatures in amorphous $Zr_3Pd$ alloys. Dashed lines indicate onset of crystallization (see text).

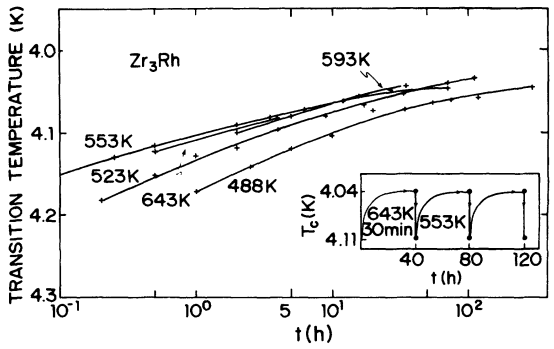


FIG. 2. Same as in Fig. 1 for amorphous $Zr_3Rh$ alloys. Note the "convergence" in $T_c$ after long term annealing. Inset shows the effect of cyclic annealing on $T_c$. The labels 643 K, 30 min, and 533 K refer to increasing and decreasing $T_c$, respectively.

Regions of $t_a$ showing tendency towards saturation in $T_c$ are indeed observed. Instability of the equilibrium structure is detected when the samples are annealed at 433 K for longer than 10 h. The transition widths $\Delta T_c$ in $Zr_3Pd$ prior to the onset of crystallization, however, are mostly 4–7 mK. This is indicative of a high degree of sample homogeneity (see Table I).

Trends of saturation in $T_c$ are also observed in $Zr_2Co$, $Zr_2Ni$, and $Zr_2Pd$ alloys, as shown in Figs. 3 and 4. On the other hand, the $T_c(t_a)$ behavior in $Zr_3Ni$ samples (Fig. 4) is rather similar to that observed in $Zr_3Pd$. Saturations in $T_c$ are only observed over short intervals of $t_a$ at 433 and 483 K. At $T_a = 593$ K (crystallization temperature at 633 K for $Zr_3Ni$),[18] strong degradation in $T_c$ ($<1.8$ K) and a significant increase in $\Delta T_c$ ($>100$ mK) are observed for $t_a > 1$ h. Again, prolonged annealing yields crystalline $\alpha$-Zr and $Zr_2Ni$ phases. It should be mentioned that the present annealing study is not performed on $Zr_3Co$ samples because $\Delta T_c > 30$ mK

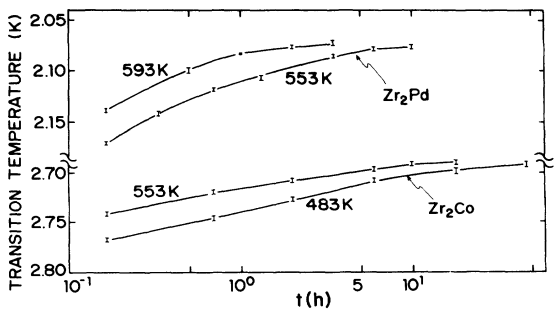


FIG. 3. Same as in Fig. 1 for amorphous $Zr_2Co$ and $Zr_2Pd$ alloys. Again, "convergence" behavior in $T_c$ is observed.

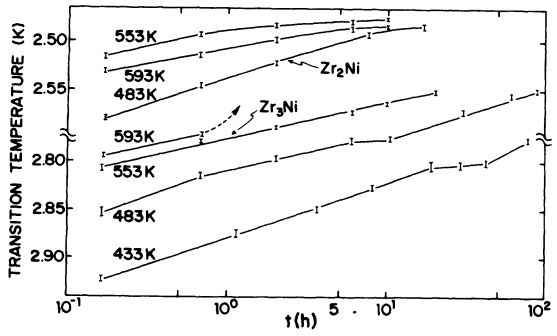


FIG. 4. Same as in Fig. 1 for amorphous $Zr_2Ni$ and $Zr_3Ni$ alloys. Note the contrasting $T_c$ trends in the two systems.

even in the as-quenched samples.

Up to this point, one naturally wonders why the equilibrium amorphous structures are stable in some systems but unstable in the others, and about the origin of the $T_c$ depression in the annealed samples. It is found from the present crystallization studies on $Zr_2X$ ($X$=Co,Ni,Pd), $Zr_3Co$, $Zr_3Ni$,[18] $Zr_3Pd$, and $Zr_3Rh$ (Ref. 17) that $\alpha$-Zr, $Zr_2Co$, $Zr_2Ni$, $Zr_2Pd$, and $Zr_3Rh$ are the stable crystalline phases. Therefore, a clear correlation is seen between the behavior in $T_c(t_a)$ and the different modes of crystallization. The latter refer to polymorphous crystallization of the amorphous alloy without any change in concentration into a supersaturated alloy or a metastable or stable crystalline compound, and eutectic crystallization defined as the simultaneous crystallization of two crystalline phases. In alloy systems undergoing polymorphous crystallization ($P$ alloys), saturation in $T_c$ is observed. On the other hand, in alloys exhibiting eutectic crystallization ($E$ alloys), no stable saturation trend can be seen. Ideally, crystallization should not occur in amorphous samples annealed below their glass temperatures. This seems to be the case in the $P$ alloys under restricted annealing time (less than 200 h) discussed earlier. The intermediate amorphous states prior to the onset of crystallization in the $E$ alloys must evolve from the "short-lived" equilibrium amorphous structures. The sharp transition $\Delta T_c$ indicates homogeneity in the intermediate states down to a scale of $\xi(0)$. Meanwhile, the tendency towards eutectic crystallization at relatively low $T_a$ suggests the presence of components (phases) with lower crystallization temperatures than in the original hosts. Ordinary x-ray scan does not indicate any observable change in the diffraction pattern. Incidentally, several cases of macroscopic phase separation in amorphous alloys were reported.[14,19,20] The present results taken together prompts one to conjecture on the possibility of microscopic phase separation in the intermediate states. The characteristic scale of the phase separation is not known at present.

In amorphous alloys post-quench annealing leads to changes in the chemical short-range order and physical short-range order of the alloys.[4] Associated with these changes are the collapse and redistribution of quenched-in voids (defects) and the reduction in internal strains. So far the $T_c$ of amorphous superconductors have been found to decrease upon annealing. Cumulated data taken from Ref. 10 and the present results include Zr-Co, Zr-Fe, Zr-Ni, Zr-Pd, Zr-Rh, La-Cu, V-Si, and Nb-Ge. This list covers a wide range of alloys with different electronic and vibrational properties. Indeed, the $T_c$ in the amorphous states can be either higher or lower than the values in their crystalline counterparts [for example, in crystalline $Zr_2Co$, $T_c \simeq 5$ K,[21] and in crystalline $Zr_3Rh$, $T_c \simeq 3$ K (Ref. 22)]. Therefore, it is unlikely that the $T_c$ depression upon annealing is due to the change in chemical (compositional) short-range order alone. In fact, it was found that the $T_c$ values of eutectic alloys depend rather sensitively on the presence of strains.[23] Therefore, the major portions of $T_c$ depression in our alloys are probably due to the "hardening" of phonon modes as the internal stress is relaxed. To account for the magnitude of $T_c$ depression ($\sim$0.2–0.5 K), a change in internal strain of $\sim$0.02% corresponding to a fractional change in phonon frequency of $\sim$0.05 is sufficient.[24] Meanwhile, modification in the chemical short-range order only has a minor effect on $T_c$. It is possible that the latter only plays an important role in determining the equilibrium $T_c$ values at different annealing temperatures. Indeed, the subtle variation in the free energy (entropy) of the structures should depend on $T_a$. Both effects can, however, participate in the reversibility process.

### C. Comparison of flux pinning force in as-quenched and annealed samples

Since the critical current $J_c$ behavior in type-II superconductors depends on the metallurgical conditions of the samples, measurement of $J_c$ can yield complementary information about the amorphous states. Here, the dependence of flux pinning behavior on annealing is studied in both $P$ and $E$ alloys. This also yields information on the homogeneity of the amorphous samples. In Fig. 5 we compare the flux pinning force $F_p$ (defined by the product $J_cH$, where $H$ is the applied magnetic field) of the $P$ alloy $Zr_2Ni$ in its as-quenched and equilibrium states. For these samples, it is found that $F_p \propto H_{c2}^{1.5}$. Taking this scaling relation into account,

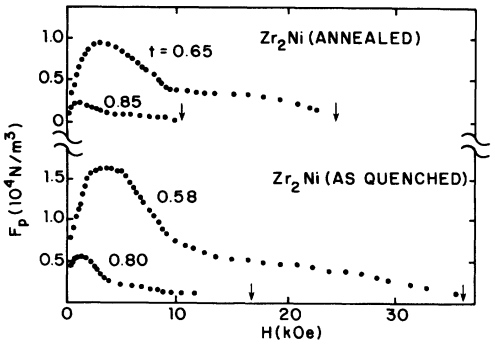


FIG. 5. Flux pinning force as a function of reduced temperature $t=T/T_c$ and applied magnetic field for $Zr_2Ni$ in the as-quenched and annealed (483 K for 17 h, $T_c=2.48$ K) states. Arrows indicate the $H_{c2}(T)$ values.

the values $F_p/H_{c2}^{1.5}$ in both states become comparable. It should be mentioned that the broad maxima observed near $H\simeq 0.1H_{c2}$ are probably due to pinning by the sample edges.[25] Electropolishing has not been able to remove this edge effect entirely. Figure 6 compares $F_p$ of the $E$ alloy $Zr_3Ni$ in its as-quenched and intermediate state. The constancy in $F_p$ as a function of $H$ is characteristic of an ideal type-II superconductor. On the other hand, it is found that $E$ alloys embedded with microcrystallites yield $F_p/H_{c2}^2$ values at least 5 times higher than the ones shown in Fig. 6. It should be mentioned that the present values of $F_p$ ($\sim 10^4$ N/m$^3$ at 1.6 K) are among the lowest reported thus far for amorphous superconductors.[26] The critical currents at $H=0$ are 100–1000 A/cm$^2$ at 1.5 K.

### D. Phase separation and the proximity effect

It was conjectured in Sec. III B that the intermediate states obtained in the $E$ alloys $Zr_3Ni$ and $Zr_3Pd$ are associated with microscopic phase separation. If

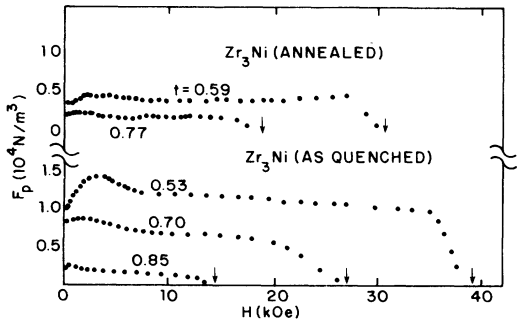


FIG. 6. Same as in Fig. 5 for as-quenched and annealed (483 K for 89 h, $T_c=2.74$ K) $Zr_3Ni$ samples.

the scale of the phase separation is smaller than the coherence length $\xi(0)$, then the sample is still homogeneous and the resistive transition can be very sharp. In general, one should investigate the transition width in samples containing different amounts of second phase(s), which can either be amorphous or crystalline. The second phases(s) might not be detectable in an ordinary x-ray scan. In what follows, a simple model based on the proximity effect will be used to study this problem.

The inset of Fig. 7 shows a section of a sample, with host parameters $T_{c2}$ and $\xi_2$, having dispersed in it a second phase with parameters $T_{c1}$ and $\xi_1$, where $T_{c2}>T_{c1}$. At some temperatures above $T_{c0}$ (temperature at which the sample resistivity vanishes) of the system, the size of the superconducting droplets $\xi$ can fit between the particles of size $a$. The $T_c$ of the droplets is still $T_{c2}$ (region $A$ in Fig. 7). As $T_{c0}$ is approached, at some point the droplets have to overlap the particles leading to a decrease in the $T_c$ of the droplets. Meanwhile, there will be a distribution in the $T_c$ of the droplets. For simplicity, we take the characteristic $T_c$ of the distribution as $T_c(B)$ found in droplet $B$ centered at one of the particles with radius equal to half of the distance $L$ between the uniformly distributed particles. Based on this simple model, the typical distribution (or

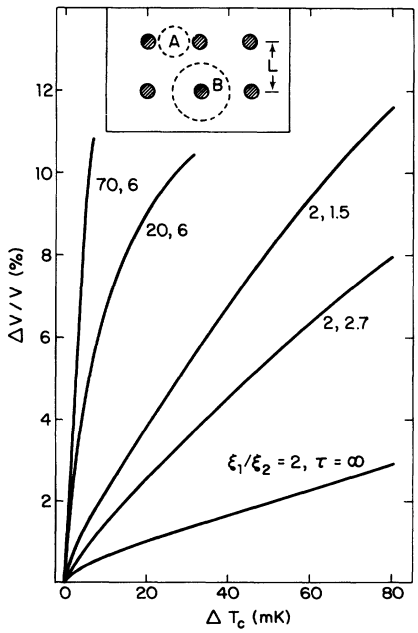


FIG. 7. Calculated fractional volume of second phase ($T_{c1}$,$\xi_1$) embedded in hose ($T_{c2}$,$\xi_2$) vs transition width for different values of $\tau=(T_{c2}/T_{c1})$ and $\xi_1/\xi_2$. Inset shows section of the sample containing inclusions (hatched circles). $A$ and $B$ represent characteristic superconducting droplets (see text).

broadening) in $T_c$ called $\gamma$ in a sample is simply taken as $T_{c2}-T_c(B)$. From previous results in inhomogeneous samples,[27] $\Delta T_c \simeq \gamma$ for small distribution in $T_c$. Therefore, we can approximate $\Delta T_c$ by $T_{c2}-T_c(B)$.

To obtain $T_c(B)$, we generalize the approach of Silvert and Singh[28] to the case $T_{c2} > T_{c1}$ and $\xi_1 \neq \xi_2$ with free boundary condition on the spherical surface of $B$. The set of equations takes the following form:

$$X(-q^2\xi_1^2)=\ln\left[\frac{1}{t}\right], \tag{2}$$

$$X(k^2\xi_2^2)=\ln\left[\frac{\tau}{t}\right], \tag{3}$$

$$\left[\frac{\xi_1}{\xi_2}\right] aq\coth(aq)-\left[\frac{\xi_1}{\xi_2}-1\right] = -ka\tan(ka+\delta), \tag{4}$$

$$\tan(kL+\delta)=-\frac{1}{kL}, \tag{5}$$

where $X(z)=\psi(\frac{1}{2}z+\frac{1}{2})-\psi(\frac{1}{2})$, $\psi$ is the digamma function, $L$ is approximated by $\xi_2\{1-[T_c(B)/T_{c2}]\}^{-1/2}$, $t=T_c(B)/T_{c1}$, $\tau=T_{c2}/T_{c1}$, $q^{-1}$ is the characteristic range of the pair correlation amplitude inside the particle, $k^{-1}$ is the wavelength of the amplitude oscillation outside the particle, and $\delta$ is the phase shift obtained from the boundary conditions. Taking $T_{c2}\simeq 3$ K, we have plotted in Fig. 7 the fractional volume of crystallites $\Delta V/V$ $[\sim(a/L)^3]$ as a function of $\Delta T_c$ for different values of $\xi_1/\xi_2$ and $\tau$. It can be seen that $T_c$ is affected by any finite size of the inclusions, contrary to the case for $T_{c2} < T_{c1}$.[28] The total transition width is simply approximated by the one due to inhomogeneities. Since the two $E$ alloy systems have very similar physical properties, we can focus our discussion on the $Zr_3Pd$ alloys. For amorphous hosts containing inclusions of second phase(s), the following special cases will be considered. A general case will be a combination of them.

(i) The inclusions are products of eutectic crystallization. Both phases $\alpha$-Zr and $Zr_2Pd$ have low $T_c$ values [$\sim$ 0.5 K for $\alpha$-Zr, $Zr_2Pd$ is not superconducting down to 1.3 K (Ref. 10)] yielding $\tau\simeq 6$ and large coherence lengths. According to Fig. 7, the transition can remain sharp as long as $\Delta V/V$ is less than several percent, since $\xi_1/\xi_2$ is quite large (estimated to be $\sim 100$ in the clean limit for the crystallites). This agrees with the present data. Meanwhile, the composition of the host remains constant so that there should be a trend towards $T_c$ saturation as the equilibrium state is approached. This is not observed. On the other hand, if the crystallites are disordered so that the ratio $\xi_1/\xi_2$ is substantially reduced, then $\Delta T_c$ should be quite large (Fig. 7). This is contrary to the experimental results.

(ii) If most of the crystallites are $Zr_2Pd$, then $T_c$ should go up as the amorphous host is enriched with Zr. Again, this disagrees with the present data.

(iii) The crystallites are predominantly $\alpha$-Zr, and the transition remains sharp according to the analysis given in case (i) (Fig. 7). $T_c$ of the host enriched with Pd will decrease with composition $x$ according to the rate $dT_c/dx = -100$ mK/at. % Pd.[10] To account for the drop in $T_c$ of up to $\sim 300$ mK below the supposedly equilibrium value (Fig. 1) would require a fractional volume of $\sim 9\%$ of $\alpha$-Zr in the host. The amount of crystallites can then be detected both in x-ray scan and flux pinning measurement (Sec. III C). As mentioned earlier, no sign of crystallization is detected. Moreover, the flux pinning forces actually decrease in the annealed samples.

Thus the picture of an amorphous host containing a random dispersion of inclusions is inconsistent with the experimental results. On the other hand, a microscopic and uniform phase separation on a scale much smaller than $\xi_2$ of the original host can still yield results which are consistent with data on transition width and flux pinning. The proximity model then becomes irrelevant. The trend of $T_c$ depression, however, is not understood at present.

## IV. SUMMARY AND CONCLUSION

In this work, we have compared the stability of equilibrium amorphous structures in eutectic and polymorphous alloys, using superconductivity as a probe. Convergent trends of saturation in $T_c$ are observed in the $P$ alloys. On the other hand, in the $E$ alloys, the $T_c(t_a)$ curves tend to diverge from each other. As a result of the evolution of equilibrium states into intermediate states, the $T_c$ values continue to decrease in the $E$ alloys. The superconducting properties of the intermediate states are characterized by sharp resistive transitions and very low flux pinning forces. This suggests that the intermediate states are highly homogeneous. More quantitative analysis of $\Delta T_c$ is carried out using a simple model based on the proximity effect. The results do not favor the picture of microcrystalline inclusions embedded in the amorphous hosts. This prompts us to conjecture microscopic phase separation in the intermediate states. The nature and scale of the phase separation deserves further structural studies of

these amorphous phases. The understanding of the stability and instability of the equilibrium amorphous structures will undoubtedly shed light on the formation of amorphous phases in general.

## ACKNOWLEDGMENT

This research is supported by the National Science Foundation under Grant No. DMR-82-02624.

[1]B. S. Berry and W. C. Pretchet, Phys. Rev. Lett. 34, 1022 (1975).
[2]T. Egami, Mater. Res. Bull. 13, 557 (1978).
[3]T. Egami, Ann. N.Y. Acad. Sci. 371, 238 (1981).
[4]T. Egami, in *Amorphous Metallic Alloys,* edited by F. E. Luborsky (Butterworths, London, in press).
[5]See, for example, Proceedings of the Twenty-Sixth Annual Conference on Magnetism and Magnetic Materials [J. Appl. Phys. 52, 1859 (1981)].
[6]M. G. Scott, Scripta Metall. 15, 1073 (1981).
[7]H. S. Chen, J. Appl. Phys. 52, 1868 (1981), and papers cited therein.
[8]A. Kursumovic, M. G. Scott, E. Girt, and R. W. Cahn, Scripta Metall. 14, 1303 (1980).
[9]A. C. Anderson, C. C. Koch, and J. O. Scarbrough, Phys. Rev. B 3, 1156 (1982).
[10]S. J. Poon, in *Amorphous Metallic Alloys,* Ref. 4, Chap. 22.
[11]A. L. Greer and J. A. Leake, in *Rapidly Quenched Metals III,* edited by B. Cantor (Chameleon, London, 1978), Vol. 1, p. 299.
[12]S. J. Poon and P. L. Dunn (unpublished).
[13]S. J. Poon, S. K. Hasanain, and K. M. Wong, Phys. Lett. 93A, 495 (1983).
[14]U. Köster (private communication).
[15]L. G. Aslamazov and A. I. Larkin, Phys. Lett. 26A, 238 (1968).
[16]J. Kübler, K. H. Bennemann, R. Lapka, S. Rösel, P. Oelhafen, and H.-J. Güntherodt, Phys. Rev. B 23, 5176 (1981).
[17]K. H. J. Buschow, J. Phys. (Paris) Colloq. 42, C8-555 (1981).
[18]Y. D. Dong, G. Gregan, and M. G. Scott, J. Non-Cryst. Solids 43, 403 (1981).
[19]C. P. Chou and D. Turnbull, J. Non-Cryst. Solids 17, 169 (1975).
[20]C. O. Kim and W. L. Johnson, Phys. Rev. B 23, 143 (1981).
[21]E. E. Havinga, H. Damsina, and P. Hokkeling, J. Less-Common Metals 27, 169 (1972), and references cited therein.
[22]A. J. Drehman and W. L. Johnson, Phys. Status Solidi A 52, 499 (1974).
[23]H. Suhl, B. T. Matthias, S. Hecker, and J. L. Smith, Phys. Rev. Lett. 45, 1707 (1980).
[24]R. E. Elmquist and S. J. Poon, Solid State Commun. 41, 221 (1982).
[25]B. M. Clemens and W. L. Johnson, J. Appl. Phys. 11, 7612 (1982).
[26]See, for example, *Proceedings of the Fourth International Conference on Rapidly Quenched Metals,* edited by T. Masumoto and K. Suzuki (The Japan Institute of Metals, 1982), Vol. II, p. 1215.
[27]S. J. Poon, Phys. Rev. B 25, 1977 (1982).
[28]W. Silvert and A. Singh, Phys. Rev. Lett. 28, 222 (1972).